Performance Characteristics of Loose-fitting Powered Air Purifying Respirators Analyzed by a Robotic Mannequin

Yoshimi Matsumura*[1], Katsumi Suzuki[1], Akio Ogawa[2] and Naoyuki Iijima[1]

[1] Technology Institution of Industrial Safety, 2-16-26, Hirose-dai, Sayama City, Saitama 350-1328, Japan.

[2] 2-3-18, Kita-urawa, Urawa-ku, Saitama City, Saitama 330-0074, Japan.

* Corresponding author and E-mail: matsumura@tiis.or.jp

ABSTRACT

A robotic mannequin was developed to measure the inward leakage (IL) of powered air purifying respirators (PAPRs) and was designed to breathe at certain levels of work rate and to drive its head and arms to move periodically. This study presents the results of the application of this robotic mannequin to practical measurements of ILs of loose fitting PAPRs (two hood types and two face-shield types).

The robotic mannequin was designed as follows: the head bent up to 30 degrees up and down in both directions from its upright position at a frequency of (17+/-1) times/min and rotated 50 degrees to the right and to the left at a frequency of (11+/-1) times/min. The upper arms moved up and down in the range between 10 and 130 degrees from the hanging position at a frequency of (7+/-1) times/min. One mode of movement of each part continued for 5 minutes and was then automatically followed by the next mode under control of a processor until the program reached the final mode. The mouth of the mannequin head was composed of an opening of concentric double tubes for inhalation and exhalation generated by a breathing machine.

Before an IL measurement started, each sample PAPR was separated into the respiratory inlet covering (RIC) and the units containing electric blower and filter, and only the RIC was examined for the IL, meaning the observed IL is different from TIL by excluding the particle penetration through filter. For the start of the examination, the robotic mannequin was placed in a NaCl aerosol chamber with a sample PAPR on its head and connected with the compressed air-line to supply air flow into the RIC of the PAPR and with an aerosol counter for monitoring the NaCl aerosol concentration in the RIC using separate tubes. The NaCl aerosol concentration in the chamber was continuously monitored with another aerosol counter throughout the measurement. As test conditions of the IL measurement using this mannequin, the breath of the mannequin was set at two work rate levels of 30 L/min and 40 L/min in sine wave form, and the air supply into the RIC was maintained at a certain flow rate varying within the range from 60 L/min to 160 L/min.

The ILs of the sample PAPRs apparently showed higher values at a work rate of 40 L/min than those at 30 L/min and showed decreasing ILs along with an increasing air supply rate, but the extents of the changes in the ILs by these test conditions varied depending on the configurations of the sample PAPRs. Among the movements of the mannequin, the head bending up and down caused an increase in

the IL of the hood-type PAPR with a short shoulder covering, and the head rotation caused an increase in the IL of a face-shield type PAPR. The movement of the mannequin's arms did not affect the ILs of the hood-type PAPR samples adopted in this study.

From the results, the robotic mannequin was considered useful to evaluate the ILs of loose-fitting PAPRs as a test method, which apparently reflected the effects of the supplied air flow rate, the breathing rate of the mannequin and the movements of the mannequin's parts on the observed ILs at certain tendencies. It could also provide information on the effective selection of loose fitting PAPRs with respect to their configuration and to the workers' movements at their worksites.

Keywords: powered air-purifying respirator, PAPR, robotic mannequin, inward leakage, IL, body movement, work rate, air flow rate

INTRODUCTION

Inward leakage (IL) is an essential property affecting the performance of loose fitting PAPRs, and the IL for each type of PAPR is most commonly evaluated by testing on human subjects. Current EN standards of loose fitting PAPRs (BS/EN12941:1998+A2:2008) and of tight-fitting PAPRs (BS/EN14972:1998+A2:2008) prescribe testing of ILs on test subjects. However, the voluntary Japanese standard 'JIS T 8157:1991; Powered air purifying respirators' adopted a mannequin with breathing function as the test equipment for ILs, although the mannequin defined by this standard had not been provided with any movable parts. Bergman M et al (Bergman M et al., 2017) recently reported a study on the penetration factors (PFs) of 3 types of loose-fitting PAPRs measured by the use of a newly developed mannequin with breathing function but no moving parts. They adopted four levels of the mannequin's work rate for the PF measurement of the sample PAPRs and the air flow was supplied by the individual sample blower respectively. As the result, PF values of the 3 samples showed a decreasing order with the increasing air supply rate, but PF values for each sample changed not in simple relation with the work rate of the mannequin. The flow rate of the air supplied by the blower was most influential to determine the PF in this study, which was big enough to supply air into the RIC to prevent significant pressure reduction in the RIC due to the breath of the mannequin.

Before 2014, there was no regulatory standard for PAPRs in Japan; in 2000, the Japanese government first investigated PAPRs to establish a regulatory standard for PAPRs. The Ministry of Health, Labour and Welfare (MHLW) trusted the investigation of PAPRs to the Technology Institution of Industrial Safety (TIIS), and a survey of PAPRs in the Japanese market at that time and of the test methods used to evaluate the functions of PAPRs were required. TIIS called scientists and PAPR manufacturers to organize a committee to perform the required investigation. During the 3-year investigation by the committee, PAPR samples purchased from the market were tested on elemental test items of PAPRs described by JIS T 8157-1991 (a voluntary standard in Japan.) and by the relevant standards of the EU and USA. The results of the study conducted by the committee were reported by TIIS as the Committee Report addressed to MHLW in March 2002 (in Japanese.)(TIIS, 2002).

Based on the 3-year investigation on PAPRs, the committee recommended development of a new IL test method using a robotic mannequin instead of human test subjects. The motivation to introduce the robotic mannequin to the IL test of PAPRs in Japan was the strong requirement for the reproducibility of the test method of IL as a standard of PAPRs. Besides, the social circumstance in Japan supported this requirement that the trained human test subjects are difficult to find for IL tests of PAPRs. The development of the robotic mannequin was managed by Mr. Kaisaburo Shigematsu, who was a committee member, and the prototype of the robotic mannequin was checked several times by the committee members before its pilot model was completed. The 1st model of a robotic mannequin with breathing function and a moving head and upper arms was completed in 2007. Soon, the IL tests of sample PAPRs were performed at the

Respirator Test Laboratory of TIIS using the robotic mannequin. The results of the tests of ILs of loose-fitting PAPRs were presented by Matsumura Y et al (2008) at the 14th International Conference of ISRP.

In 2009, JIS T 8157:1991 was revised to JIS T 8157:2009, in which the IL test method using the robotic mannequin developed in 2007 and completed as the test equipment by SIBATA Scientific Technology Ltd. (Type PR-01, SIBATA, Japan) was adopted prior to the establishment of the government regulatory standard. This standard was referred to as a voluntary standard by manufacturers and users in Japan before the Japanese government regulatory standard was issued in 2014.

MHLW of the Japanese government moved to prepare the regulatory standard of PAPRs in 2009 based on the investigation conducted by the preceding committee on PAPRs and with the developed robotic mannequin as the IL test method. After a few revisions of the standard draft, the regulatory standard of PAPRs (MHLW, Ministerial Notification No. 455, November 28th, 2014) was issued in 2014 by MHLW, and the national approval system of PAPRs was enacted at the same time.

Thus, in Japan, the robotic mannequin is currently authorized as the test equipment for the examination of ILs of PAPRs by JIS T 8157 (2009) and by the government regulatory standard of PAPRs (2014).

This study was designed in 2007 to ascertain how ILs of loose fitting PAPRs could be observed by the use of the robotic mannequin and to examine the effects of the operational conditions of the robotic mannequin on the ILs of sample PAPRs. For this purpose, four types of loose-fitting PAPRs were submitted to the IL examination against NaCl aerosol using the robotic mannequin under various conditions of its movement and breathing rate, as well as under varying air flow rates supplied into the RIC of the sample from the laboratory compressed-air line. In this experimental scheme, the unit containing an electric blower and particle filters was removed from the sample PAPR, and clean air was supplied into the RIC of PAPR at controlled flow rates. Consequently, the observed IL did not contain particles penetrating through filters into the RIC of the samples.

METHODS

Configuration of the Robotic Mannequin and Its Motion Program

The robotic mannequin used in this study had the configuration shown in the schematic diagram in Figure 1. The head form was the same as that adopted in the Japanese Government Standard of Particulate Respirators (Ministry of Labour, Ministerial Notification No. 19-1988), which was mounted on a torso of a standard Japanese male body. The dimensions of this head form were based on Japanese male facial data reported by the Aero-medical Research Laboratory, Japan Air Self-Defense Force (1972). The mouth opening in the head form was composed of a concentric double tube, the inner tube of which was connected to the breathing machine in inspiration mode, and the outer tube was connected to the same machine in exhalation mode. The open and closed positions of the air-flow line were switched by the two in-line diaphragm valves. Upper arms were attached to each side of the shoulder.

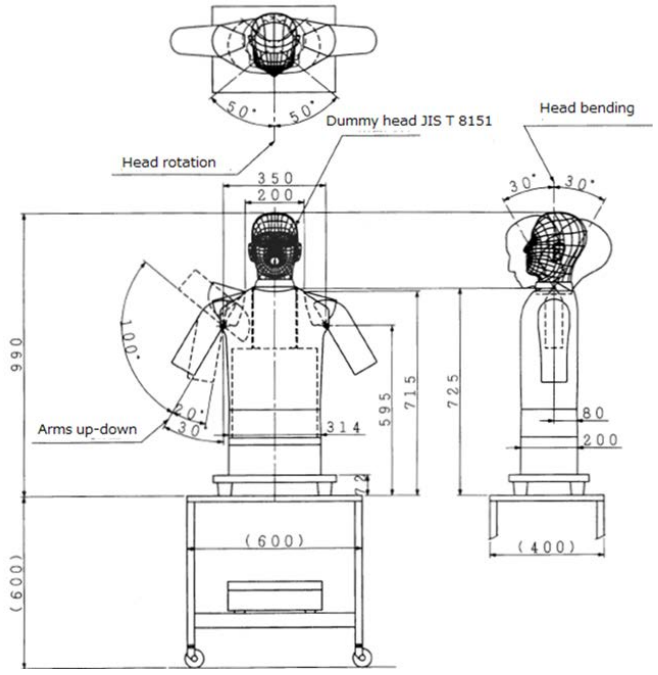

Figure 1. Schematic diagram of the robotic mannequin.

The head form could bend 30 degrees up and down in both directions from its upright position at a frequency of (17+/-1) times/min, and could also rotate 50 degrees to the right and to the left at a frequency of (11+/-1) times/min. Both upper arms could be raised out to the sides in the range between 10 and 130 degrees at a frequency of (7+/-1) times/min. The modes of movements of these parts of the mannequin driven by the programmed servomechanism are shown in Table I, and the photographs of the mannequin in four modes are shown in Figure 2.

Table I. Modes of the Servo-Mechanical Movements of the Robotic Mannequin

Mode No.	Head	Arms	Range of motion of moving part	Frequency (time/min)
1	Rest at upright position	Rest at 10° from the hung position by side	-	-
2	Bending up and down		30˚ up and down from upright position	17±1
3	Rotation to the right and to the left		50˚ to the right and to the left from the right angle of the face	11±1
4	Rest at upright position	Moving up and down	Moving arms from 10˚ to 130˚ from vertically hung position	7±1

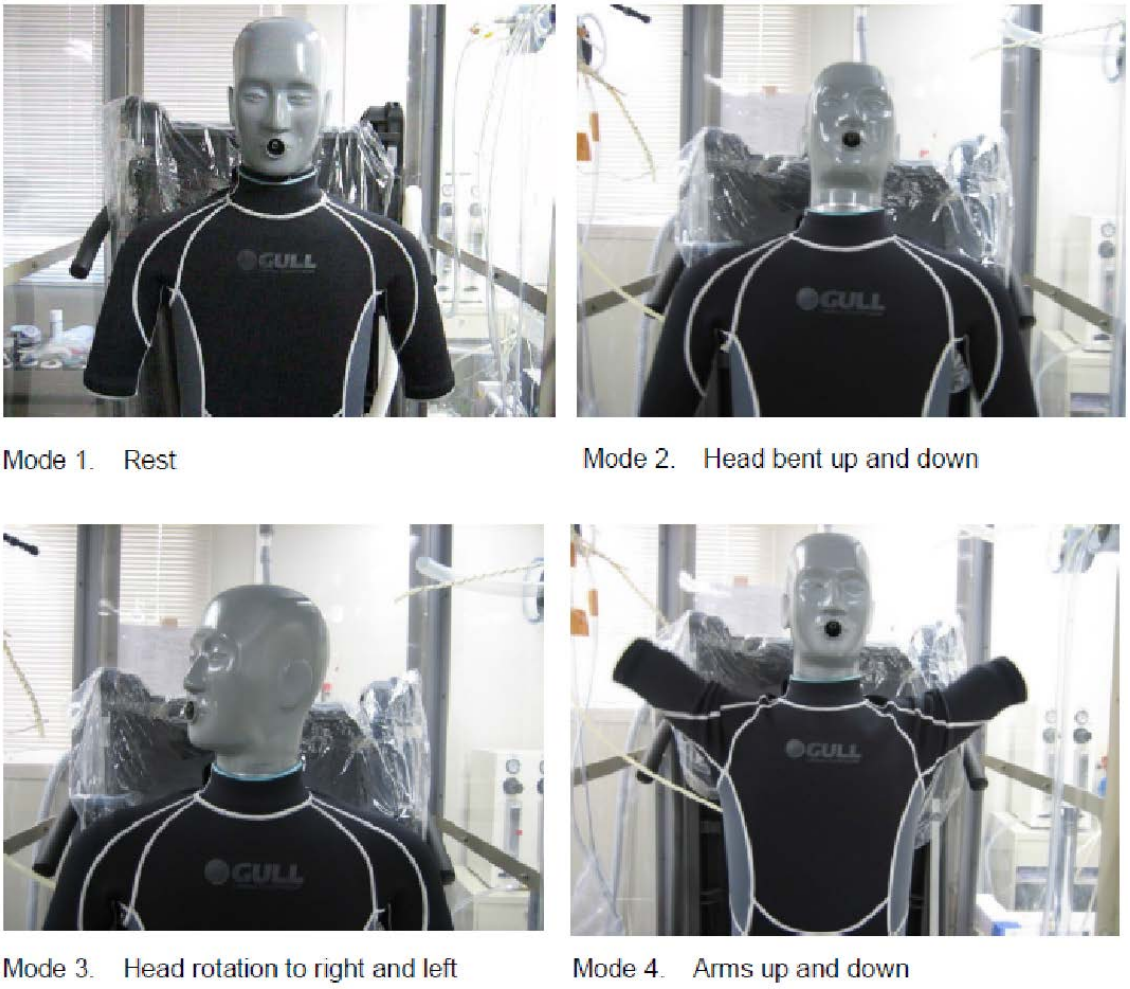

Figure 2. The mannequin in four modes of movement:
Mode 1: Rest
Mode 2: Head bending up and down
Mode 3: Head rotation to the right and to the left
Mode 4: Arms up and down

The servo-controlled breathing simulator of Type KBS-03 (Koken Ltd., Japan) was used to generate the breath of the mannequin in sine wave form at two breathing rates of 30 L/min and 40 L/min, as shown in Table II. The breathing simulator consisted of two servo-controlled cylinders and a processor that could generate breath at a certain flow rate and with a certain flow pattern, which could realize any breathing patterns memorized by the processor (Yuasa H et al, 2008). In the exhalation phase of the breath, the air exhaled from the breathing machine passed to the outer tube of the concentric double tube of the mannequin and was exhausted into the RIC of the sample PAPR, and in the inhalation phase, the air inside the RIC was drawn through the inner tube of the concentric tube and passed to the breathing machine.

Table II. Respiration Conditions Generated by the Breathing Apparatus

Breathing Condition	Volume of a breath	Number of breaths/min	Breathing rate	Peak flow rate of a sine wave
Standard	2.0 liters	15 breaths/min	30 liters/min	94.2 liters/min
Heavy	2.5 liters	16 breaths/min	40 liters/min	125.6 liters/min

Structure of the Test Apparatus and Conditioning for the Inward Leakage Test

The robotic mannequin was placed in an exposure chamber with a size of 1 m width, 2 m depth and 2 m height and exposed to NaCl aerosol. NaCl aerosol was generated from 2% NaCl solution by a generator placed outside the chamber, introduced into the chamber from one of its upper corners close to the chamber ceiling at 300 L/min, and distributed into the chamber through a punched board which was fixed at 5 cm lower than the ceiling to produce down-flow to obtain a homogeneous dispersion. The atmospheric air inside the chamber was stirred by a small fan placed on the chamber floor at a distance of approximately 1 m away from the mannequin face to generate a wind of approximately 0.5 m/s onto the mannequin face. The pressure in the chamber was maintained at -10 to -20 Pa lower than that of the room atmosphere to prevent the leakage of aerosol out of the chamber. NaCl aerosol in the chamber was characterized by SMPS (Model 3080 & Model 3022A, TSI, Minnesota), whose particle size distribution was represented by the count median diameter of 0.08 μm with a geometric standard deviation of 1.86. The concentration of NaCl was in the range of 8 - 9 mg/m^3, as measured by gravimetric analysis at the start of daily measurement and then monitored continuously with an MT-9100 (SIBATA Scientific Technology Ltd., Japan), a calibrated digital aerosol counter of scattered light photoelectric meter type throughout the IL measurement. Another MT-9100 digital aerosol counter was used to monitor the aerosol concentration in the RIC of the PAPR sample during the IL measurement. These aerosol counters integrate the scattered light for one minute, and output the counts every one minute respectively.

The gravimetric analysis of the aerosol concentration was carried out as follows. Through a high efficiency glass fiber filter of 110 mm in diameter supported by a holder, the chamber air was drawn at 85 L/min for 5 min. The weight difference of the filter measured before and after the air drawing was the weight of NaCl (ΔW, mg) contained in the air drawn through the filter. The aerosol concentration (Co, mg/m^3) was calculated by Eq. 1.

$$C_0 = \frac{\Delta W \times 1000}{85 \times 5} \qquad \text{Eq. 1}$$

Two MT-9100 instruments (No. 1 for monitoring the chamber air and No. 2 for monitoring the air inside the RIC of a PAPR sample) were calibrated simultaneously with the gravimetric analysis of NaCl aerosol concentration by the following procedure. First, clean air was drawn through the two respective MT-9100 instruments, and the digital counts (B1 and B2) were recorded as the background levels of the instruments. Then, the air in the chamber containing NaCl aerosol was simultaneously drawn through the two instruments individually at 2 L/min, and the digital counts were recorded as D1 and D2. From these data, the correlation factor (K) of the sensitivity of MT-9100 (1) against that of MT-9100 (2) was calculated by Eq. 2.

$$K = \frac{D1 - B1}{D2 - B2} \qquad \text{Eq. 2}$$

For continuous monitoring of the aerosol concentration in the chamber, the digital output of MT-9100 (1), noted as Ei measured during the measurement, can be converted to the gravimetric concentration, Ci (mg/m^3), with the following Eq. 3 in which $\frac{C0}{(D1-B1)}$ was the conversion coefficient between

the digital count of MT-9100 (1) and the gravimetric concentration. Thus, the gravimetric concentration of Ci (mg/m^3) in the chamber was derived by Eq. 3 from the digital count of Ei.

$$Ci = (Ei-B1)\times\left(\frac{Co}{D1-B1)}\right) \qquad \text{Eq. 3}$$

When the IL measurement was performed for a test condition and MT-9100 (1) and MT-9100 (2) showed the respective digital counts of F1 and F2, the IL(%) was calculated by Eq. 4.

$$IL = K\times\left(\frac{F2-B2}{F1-B1}\right)\times 100 \qquad \text{Eq. 4}$$

For the testing of IL of a loose-fitting PAPR, a sample PAPR was placed on the head form of the mannequin, and an air flow line from the compressor outside the chamber was connected to the hose of the sample RIC of PAPR. The air flow was sent into the RIC of the sample through the air line with an in-line HEPA filter from a compressor and maintained at a constant flow rate with a mass flow controller during a series of movements of the mannequin. The air inside the RIC of the worn PAPR was sampled through the inhalation tube of the mannequin, the air outside the PAPR was sampled outside the RIC approximately 50 cm away from the mannequin head, and then the two air samples were sent through two tubes to the two respective MT-9100 aerosol counters (1) and (2) placed outside the chamber. The flow diagram of the IL test apparatus is shown in Figure 3.

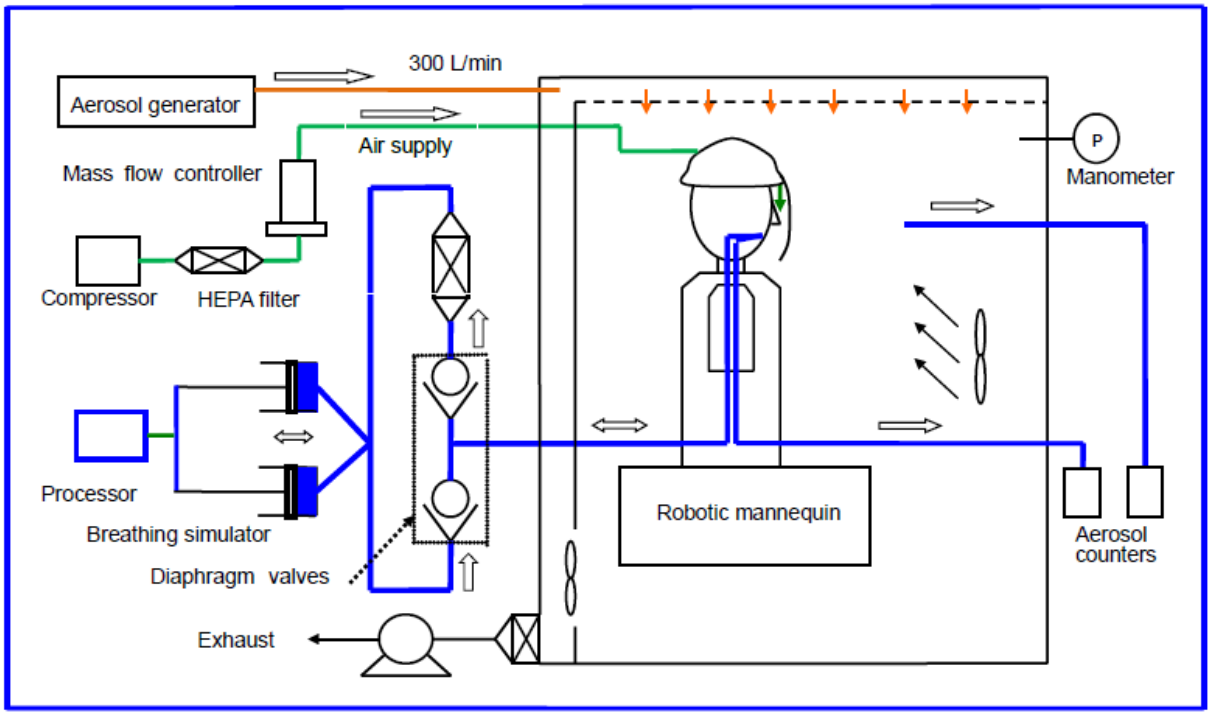

Figure 3. Flow diagram of the inward leakage test apparatus with use of robotic mannequin.

Loose-fitting PAPRs as the Samples of This Study and Their Test Conditions

Four types of loose fitting PAPRs shown in Table III, which were purchased in the market in 2008, were submitted to the IL examinations in this study. The chosen samples were two hood types and two face-shield types. The reason for choosing these devices as the samples for this study was that these devices were popular among Japanese workers, and they were designed for the most common uses in 2008 expected for loose-fitting PAPRs in Japan. The appearances of the samples are shown in Figure 4.

The manufacturers of the sample PAPRs had been informed of the submission of these PAPR devices to the IL examination with use of the robotic mannequin method and gave their consent. The powered blowers attached to the sample PAPRs were removed, and only the RICs were used as the samples for this study. The compliance of the structures and properties of these PAPR devices against JIS T 8157-1991 were the responsibilities of the manufacturers themselves because in 2008, the government regulatory standard on PAPRs had not been established.

Table III. Loose-fitting PAPR Samples and Applied Test Conditions

Sample ID	Product name[1)]	Manufacturer	Applied mode no.	Air flow rate[2)] (L/min)
Hood A	EC Hood	Shigematsu Works Co., Ltd.	1, 2, 3, 4	60-120 / 80-138
Hood B	LS-350FNL	Yamamoto Kogaku Co., Ltd.	1, 2, 3, 4	60-120 / 80-138
Faceshield A	SAM-AP	Shigematsu Works Co., Ltd.	1, 2, 3	80-138 / 104-160
Faceshield B	LS-350WL	Yamamoto Kogaku Co., Ltd.	1, 2, 3	80-138 / 104-160

Notes:

1) Product name identifies the configuration of the RIC of the PAPR sample but does not include the original powered blower with filters belonging to the PAPR sample.

2) Air flow rate indicates that of the air flow supplied by the compressed air line into the sample RIC. The smaller flow rate range was applied to the standard work rate condition (30 L/min) of the mannequin, and the larger flow rate range was applied to the heavy work rate condition (40 L/min).

Figure 4. Photographs of the loose fitting PAPRs submitted to the IL test in this study.

Procedure of Inward Leakage Testing of PAPRs with a Robotic Mannequin

The RIC of a sample PAPR was put on the head form of the mannequin placed in the chamber, and the air supply hose was connected to the compressed air line. The air flow supplied from the compressed air line was adjusted to a flow rate of 60 L/min, 80 L/min, 104 L/min, 120 L/min, 138 L/min or 160 L/min, as shown in Table III. The breathing condition of the mannequin was set at the standard work rate (30 L/min) or at the heavy work rate (40 L/min). The NaCl aerosol concentrations inside and outside the RIC of the sample PAPR were monitored by the two aerosol counters, for which the air from inside and from outside the RIC of the sample PAPR were drawn at a flow rate of 2 L/min, and the two aerosol concentrations were recorded every minute.

After 3 minutes of preconditioning of the test apparatus with the air supply and the breathing of the mannequin, the movements of the mannequin and the IL measurement started. The mannequin movement started in Mode 1 and proceeded in the order of the mode number shown in Table I to the final Mode 4 for hood-type PAPRs, and from Mode 1 to the final Mode 3 for face-shield-type PAPRs. In the program, each mode continued for 5 minutes, and after one mode ended, Mode 1 was inserted for one minute before proceeding to the next Mode. Consequently, 5 data points of IL were obtained for each mode under certain test conditions of the work rate and the air flow rate. The IL rate was calculated from the digital counts of the two aerosol counters every 1 minute by Eq. (4), and the average and standard deviation of the measured 5 data points were derived for each test condition.

RESULTS

The ILs of the four loose-fitting PAPRs put on the robotic mannequin were measured under test conditions of breathing rate, moving mode of the mannequin and air flow rate supplied from the compressed air line. To determine the IL rate of each of the sample PAPRs under each test condition, the arithmetic mean and the standard deviation were calculated across the 5 data points, which are shown in Table IV. Figure 5 shows all data of ILs observed on face-shield B for each mannequin movement from Mode 1 to Mode 3 at the heavy breathing rate of 40 L/min and at the air flow rates of 104 L/min, 120 L/min, 138 L/min and 160 L/min. The numerals 1, 2 and 3 on the plots denote the mode of the mannequin movement. In the test of the two face-shield-type samples, Mode 4 of the mannequin movement was not applied because the movement of the arms did not exert significant influence on the IL for hood-type PAPRs, and this result suggested that no significant influence was expected on the face-shield-type PAPRs with no parts covering the shoulders.

As shown in Figure 5, the fluctuation of the IL was observed among the 5 data points measured under certain test conditions. This might be caused by the periodic movements of the mannequin and the sine wave form of the mannequin's breath, which were controlled at different frequencies, and might cause irregular changes in the air flow patterns in the RIC during the time course of 5 minutes. The IL of face-shield B presented in Figure 5 shows apparent changes in IL in relation to the changes in the test conditions: that is, the IL was decreased by the increasing air flow rate and was increased in Modes 2 and 3 of the mannequin movements at air-flow rates of 120 L/min, 138 L/min and 160 L/min respectively. At the lowest air flow rate of 104 L/min, the highest IL in the range between 2.96%-3.14% was observed in all of the examined modes of the mannequin movement. At the flow rate of 160 L/min, the observed IL rate remained in the lowest range between 0.62 and 0.70%, with a slight increase for Modes 2 and 3 of the mannequin movement.

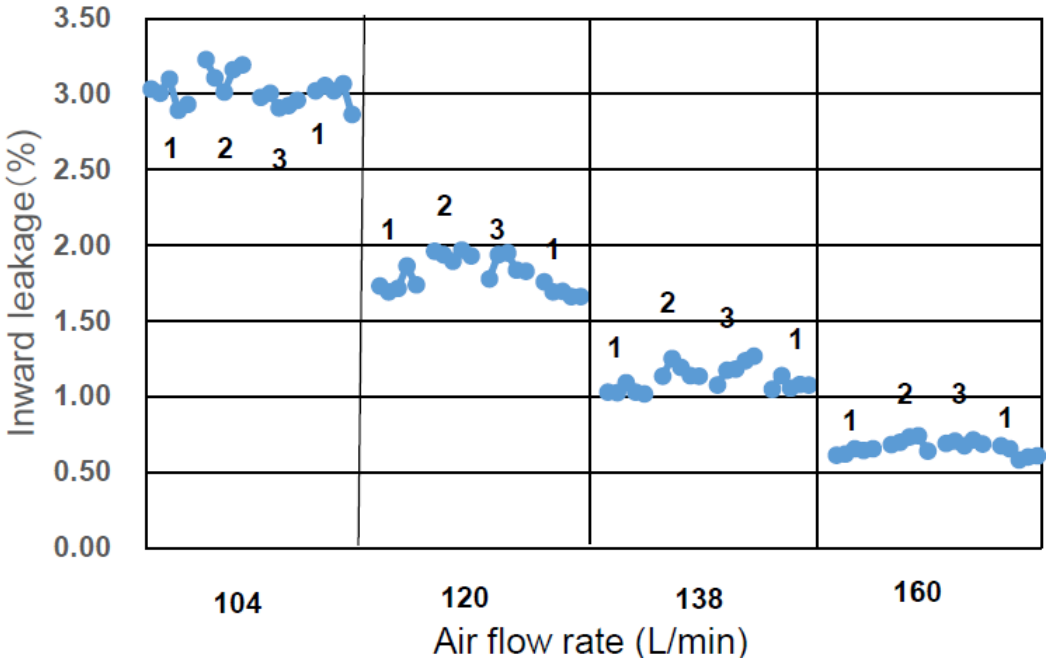

Figure 5. Inward leakage rate (%) observed on face-shield B during the program of mannequin movements from mode 1 to mode 3 at four air flow rates and with the heavy breathing condition.

Table IV summarizes the inward leakage rate (%) of PAPR samples for each test condition of mannequin movement, air flow rate and breathing condition. The ILs were presented by the average and the standard deviation of 5 data points observed at each test condition.

Figure 6 to Figure 9 show the observed IL rates of the four PAPR samples in relation to the test conditions of the mode of mannequin movement, the breathing rate and the air flow rate. Here, the IL rate under each test condition is represented by the average of the 5 observed plots shown in Table IV.

From the results shown in Figure 6 to Figure 9, the IL values of the four types of loose-fitting PAPRs showed the common tendency to increase the IL in the lower air flow rate range. The observed IL on hood A showed that the air flow rates close to the peak inhalation rates of the mannequin's breath, i.e., 94.2 L/min for a normal breathing rate and 125.6 L/min for a heavy breathing rate (shown in Table II), were the critical flow rates to keep the air inside the RIC away from contamination by the outside air. These results can be explained by the possible negative pressure inside the RIC produced by the peak inhalation of the mannequin, which could not be compensated by the air flow supplied from outside.

Figure 7 shows the IL of hood B observed in the normal and heavy breathing conditions. The IL showed only a small increase in the lower air flow rate range. This sample includes a long hood covering the mannequin's shoulders, which might prevent the back flux of atmospheric air into the hood induced by the peak inhalation of the mannequin.

Figures 8 and 9 show more intensive effects of air flow rate on the ILs of face-shield-type PAPRs. These results showed that, for face-shield-type PAPRs, the air flow supplied at the flow rate nearly corresponding to the peak inhalation of the mannequin's breath, i.e., 94.2 L/min for a normal breathing rate and 125.6 L/min for a heavy breathing rate, were insufficient to maintain the IL at low levels. The air flow supplied at a far higher flow rate seems necessary to provide effective respiratory protection, especially when the wearer's head moves.

Table IV. Observed Inward Leakage Rates of PAPR Samples at each Mannequin Mode and Air-supply Rate (n = 5)

PAPR sample	Breathing condition		Air supply rate, L/min	Robotic mannequin mode									
	Volume of a breath, L	Breath no./min		1 Rest		2 Head bending		3 Head rotation		4 Arms up & down		1 Rest	
				Average	STD	Average	STD	Average	STD	Average	STD	Average	STD
Hood A	1.5	20	60	0.87	0.042	3.65	0.321	1.55	0.114	0.87	0.090	0.73	0.056
			80	0.02	0.011	0.06	0.014	0.02	0.006	0.02	0.004	0.02	0.004
			104	0.02	0.000	0.02	0.007	0.02	0.004	0.02	0.003	0.02	0.003
			120	0.01	0.003	0.01	0.003	0.01	0.007	0.01	0.003	0.01	0.006
Hood A	1.6	25	80	0.37	0.018	2.03	0.201	1.14	0.163	0.46	0.073	0.39	0.037
			104	0.03	0.003	0.12	0.018	0.06	0.007	0.03	0.004	0.04	0.005
			120	0.02	0.004	0.02	0.006	0.03	0.003	0.04	0.006	0.03	0.006
			138	0.02	0.000	0.02	0.008	0.02	0.003	0.02	0.006	0.02	0.000
Hood B	1.5	20	60	0.36	0.028	0.40	0.015	0.47	0.033	0.32	0.046	0.34	0.012
			80	0.22	0.021	0.28	0.008	0.42	0.028	0.18	0.077	0.17	0.011
			104	0.09	0.006	0.15	0.014	0.23	0.034	0.07	0.024	0.08	0.008
			120	0.04	0.004	0.08	0.009	0.13	0.006	0.03	0.003	0.04	0.003
Hood B	1.6	25	80	0.27	0.011	0.35	0.020	0.40	0.035	0.27	0.024	0.28	0.010
			104	0.20	0.008	0.26	0.015	0.30	0.013	0.15	0.029	0.19	0.005
			120	0.12	0.005	0.18	0.012	0.22	0.011	0.08	0.014	0.12	0.004
			138	0.08	0.008	0.15	0.011	0.18	0.027	0.07	0.010	0.09	0.007
Face shield A	1.5	20	80	2.06	0.059	2.25	0.099	3.33	0.097	-	-	2.28	0.135
			104	0.82	0.016	0.82	0.035	1.11	0.000	-	-	0.83	0.050
			120	0.39	0.008	0.40	0.019	0.51	0.007	-	-	0.36	0.038
			138	0.16	0.004	0.18	0.012	0.21	0.002	-	-	0.18	0.000
Face shield A	1.6	25	104	2.58	0.050	2.53	0.041	3.24	0.230	-	-	2.42	0.105
			120	1.29	0.042	1.39	0.021	1.65	0.030	-	-	1.31	0.028
			138	0.67	0.017	0.75	0.035	0.81	0.012	-	-	0.68	0.016
			160	0.31	0.008	0.35	0.017	0.36	0.014	-	-	0.32	0.013
Face shield B	1.5	20	80	3.04	0.162	3.18	0.141	2.93	0.096	-	-	2.88	0.077
			104	1.21	0.039	1.41	0.022	1.40	0.034	-	-	1.24	0.071
			120	0.57	0.022	0.76	0.028	0.77	0.049	-	-	0.62	0.040
			138	0.37	0.018	0.48	0.012	0.47	0.024	-	-	0.37	0.013
Face shield B	1.6	25	104	2.99	0.081	3.14	0.083	2.96	0.041	-	-	3.01	0.081
			120	1.75	0.067	1.94	0.028	1.87	0.075	-	-	1.69	0.040
			138	1.04	0.031	1.17	0.052	1.19	0.072	-	-	1.08	0.035
			160	0.64	0.020	0.70	0.014	0.69	0.015	-	-	0.62	0.039

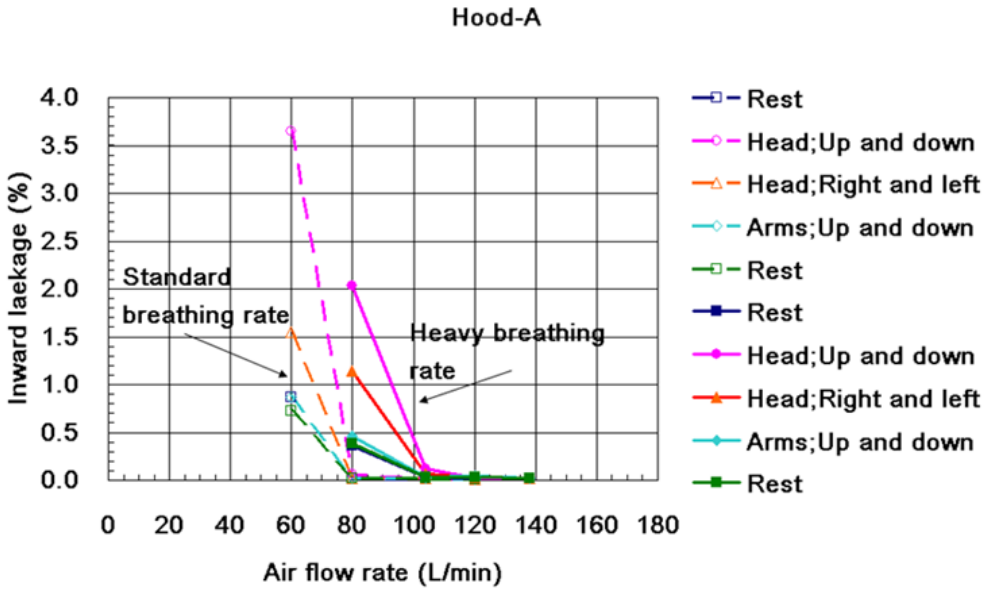

Figure 6. Inward leakage (%) of hood A observed for each mode of mannequin movement in relation with the breathing rate and the air flow rate (Air flow rate range: 60 to 120 L/min at a standard breathing rate; 80 to 138 L/min at a heavy breathing rate).

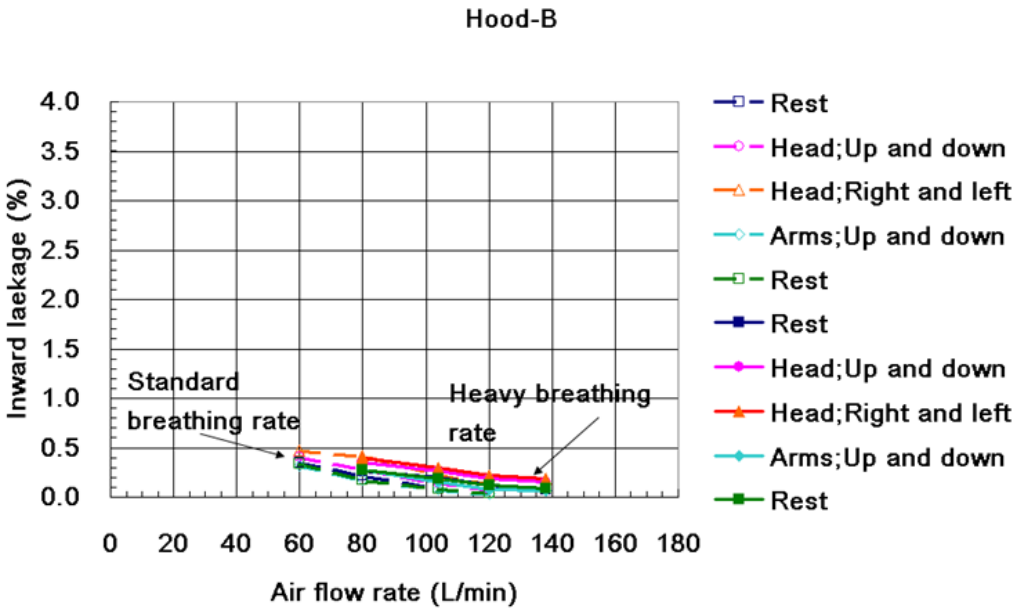

Figure 7. Inward leakage (%) of hood B observed for each mode of the mannequin movement in relation with the breathing rate and the air flow rate (Air flow rate range: 60 to 120 L/min at a standard breathing rate; 80 to 138 L/min at a heavy breathing rate).

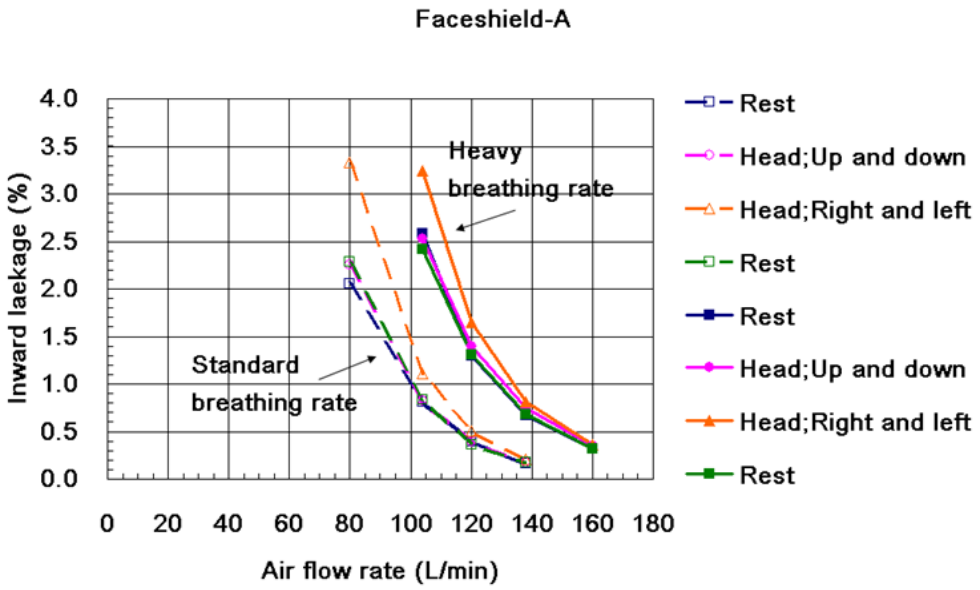

Figure 8. Inward leakage (%) of face-shield A observed for each mode of mannequin movement in relation with the breathing rate and the air flow rate (Air flow rate range: 80 to 138 L/min at a standard breathing rate; 104 to 160 L/min at a heavy breathing rate).

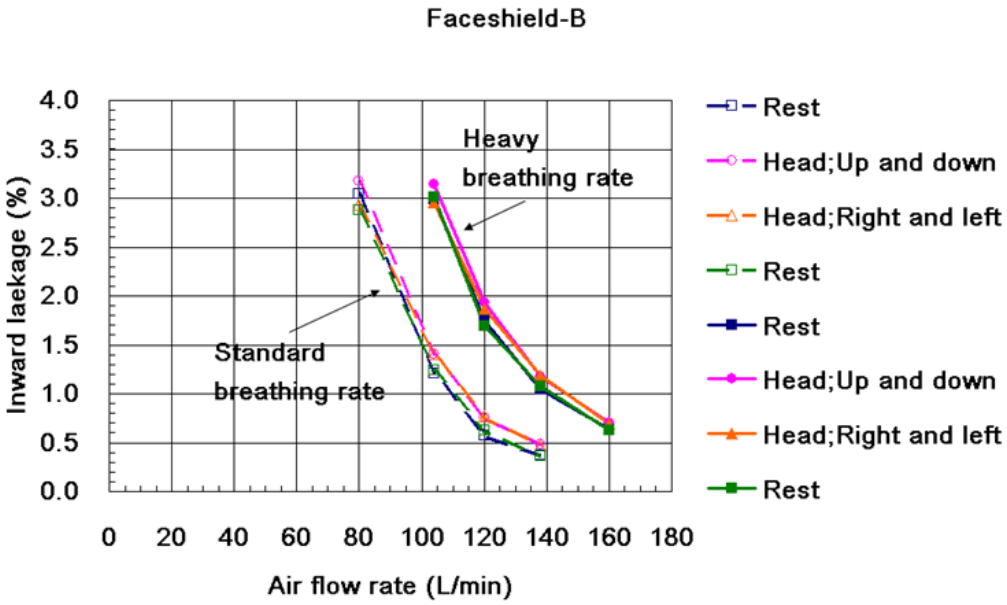

Figure 9. Inward leakage (%) of face-shield B observed for each mode of mannequin movement in relation with the breathing rate and the air flow rate (Air flow rate range: 80 to 138 L/min at a standard breathing rate; 104 to 160 L/min at heavy a breathing rate).

Among the modes of the mannequin's movement, moving the head up and down most intensively gave rise to the IL for hood A, followed by the head rotation. This may be related to the short length of the hood of this sample, which did not cover the mannequin's shoulders, and the fact that the seal between the hood and the mannequin's face or neck might be broken by the head motion. In hood B, the IL did not significantly increase in the lower air flow rate range, and the IL was kept at low levels throughout the range of air flow rates. Hood B has a longer hood covering the mannequin's shoulders, which might be effective to prevent the air flux from outside into the RIC caused by the inhalation of the mannequin.

For face-shield type PAPRs, the head rotation to the right and to the left caused the most intensive increase in the IL among the 3 modes of the mannequin for face-shield A. The exact air flow rate necessary for each face-shield-type PAPR to maintain the IL at a safe level seems dependent on the configuration of the face-shield and the movement of the user's head.

The results of the examinations of the IL values of loose-fitting PAPRs performed under various operational conditions in this study are summarized as follows.

1. For all PAPR samples, the lower air flow rate supplied from the compressed air line tended to increase the ILs, even in the resting mode of the mannequin. The air flow rate supplied from outside into the RIC was the most influential factor to keep the IL at lower levels for the four PAPR samples examined in this study. The necessary air flow rate to keep the IL lower than a certain required level depends on the breathing condition of the mannequin and the configuration of the PAPR.
2. The heavy breathing condition of the mannequin caused higher ILs than the standard breathing condition at the same air flow rate. This tendency occurred more intensively in face-shield-type PAPRs than in hood-type PAPRs. For face-shield-type PAPRs, the higher rate of the air flow supplied from the compressed-air line was more necessary than for hood-type PAPRs to keep the IL at the same low level.
3. Among the modes of movement of the robotic mannequin, head rotation to the right and to the left caused the greatest increase in the IL of face-shield-type PAPRs, and head bending up and down caused the greatest increase for hood-type PAPRs, though the extent of the effect differed depending on the configuration of the RIC.
4. This study proved that IL measurement by the robotic mannequin could verify whether the air flow rate supplied by the intrinsic blower is satisfactory to keep the IL lower than a set criterion at the preset breathing rate of the mannequin. Moreover, the test conditions can be reproduced by the control of the mannequin. This is taken as an advantage of IL examination with the robotic mannequin over that with human test subjects. The movements of the mannequin's head and arms are also controlled by a program and can be reproduced. For these reasons, the robotic mannequin was proved to be useful to evaluate the performance of PAPRs with respect to inward leakage.

The results also showed that the robotic mannequin could provide useful information on the performance characteristics of PAPRs in relation to the configuration of PAPRs and the motions of the PAPR wearers at worksites.

DISCUSSION

The robotic mannequin was introduced into the Japanese government regulatory standard of PAPRs issued in 2014 (Ministry of Health, Labour and Welfare, Ministerial Notification No.455, 2014), and the inward leakage of PAPRs is evaluated according to this standard in the approval test of PAPRs performed by TIIS and also in the test at manufacturers' laboratories.

For the examination of IL of PAPRs using the robotic mannequin, the breathing condition of the mannequin is the most critical factor for the resultant ILs. In the current regulatory standard of Japan, two breathing rates of 30 L/min and 40 L/min are defined, which cover most of the Japanese workers' work

rates classified as light work, moderate work and some of the heavy work defined as Classes 2, 3 and a part of Class 4 by ISO/TS 16976-1 (2015) but do not cover the heavier work defined as Classes 4 and 5 by the same ISO/TS. Haruta et al (Haruta H et al, 2012) surveyed the breathing rates of 150 Japanese workers at 10 workplaces of an electrical wire manufacturing company and reported that the average breathing rate of the workers in eight workplaces was lower than 30 L/min, although they found a few workers whose breathing rates exceeded 30 L/min in one workplace and exceeded 40 L/min in another workplace. In the examination of the IL according to the standard, the blowers belonging to the PAPR is conditioned at the minimum designed air flow rate. So, the user of a PAPR whose work rate might be classified as heavy or very heavy is required to ascertain whether the air flow rate supplied by the blower can cover his breath by referring to the manufacturer's instruction or any other information provided by the manufacturer of the PAPR. In practice, the Japanese regulatory standard of PAPRs includes the specifications of the air flow rate supplied by the blower larger than 104L/min for standard flow rate type and larger than 138L/min for heavy flow rate type of loose-fitting PAPRs and no specification for the air flow rate supplied by the blower for the tight-fitting PAPRs, because tight-fitting PAPRs with breath-responsible type supply the air not at a certain flow rate but at the variable flow rate coping with the wearer's breath to keep a certain positive pressure in the RIC in use. So, the IL examination is an important test to prove if the blower can supply enough air flow into the RIC to protect the air inside the RIC from contamination.

The IL test procedures described in EN12941 and EN12942 require the test subject to walk at 6 km/h with speaking and moving his head. This exercise may be classified as Class 4 'Heavy work' presented in Table A.1 of ISO/TS 16976-1 Annex A, corresponding to the minute volume of 44 L/min, which is heavier than the work rate of 40L/min realized by the robotic mannequin conditioned at a heavy work rate in this study.

The IL measurement using the robotic mannequin specified the effect of each mode of head movement on the IL of the sample PAPRs. The up and down movement of the head increased the IL of hood A in this study but did not induce a significant change in the IL of hood B. Head rotation to the right and to the left increased the IL of face-shield A but did not have a substantial effect on face-shield B. The up and down movement of the arms did not show any effect on the ILs of hood-type samples, and this result suggested no possibility of the same mode to affect the ILs of face-shield type PAPRs. However, the movement of arms of the robotic mannequin is still a necessary function of the robotic mannequin for the examination of such PAPRs with longer hood covering the wearer's shoulders. The present model of a robotic mannequin has not any other movement, but the authors have no reason to eliminate any other motions in future.

Thus, evaluation of the performance of a type of PAPR with this robotic mannequin would provide valuable information on the characteristics of the PAPR, suggesting the possible occurrence of high IL during practical use or with special movements of the wearer at worksites. It would also help the manufacturer to improve their products to be compatible with use.

Since 2014 when the Japanese government regulatory standard for PAPRs was issued and the national type-specific approval system for PAPRs started, there exists no special problem or claim against the IL examination by the use of the robotic mannequin. Moreover, this method has solved the difficult problem in Japan to find trained test subjects for the performance examination of respiratory protective devices. Further investigation to characterize the IL test method using the robotic mannequin seems necessary in comparison with the method using human test subjects.

CONCLUSIONS

The robotic mannequin was developed as equipment for the examination of ILs of PAPRs as a substitute for human test subjects and was applied to the IL measurements of 4 types of loose-fitting PAPRs in this study. The robotic mannequin can move its head and arms periodically, and can breathe in sine wave form through the mouth aperture by the connected breathing simulator. The examinations of the ILs of 2 hood-type PAPRs and 2 face-shield-type PAPRs were carried out at 2 levels of breathing rate of the mannequin and at 5 levels of air flow rate supplied from a compressed air line, and the results showed that the IL test method with the robotic mannequin is useful for providing information on the performance of PAPRs with certain relations with the test conditions. The test conditions can be artificially defined and are reproducible, which are advantages of the mannequin over the human test subjects.

However, the robotic mannequin provides only simplified test conditions for IL measurement, especially with respect to the modes of movement of the head and arms. Further investigation on the robotic mannequin is expected to explore the possibility of mechanical test method in comparison with the test with human subject.

Acknowledgements

The authors would like to note the innovative spirit of Mr. Kaisaburo Shigematsu in constructing the 1st model of the robotic mannequin by request of the government committee ‘Studies on PAPRs’ in 2000 to 2002. The authors are grateful to the technical staff of SIBATA Scientific Technology Ltd., who completed the robotic mannequin as test equipment applicable to routine examination of PAPRs. The authors thank all of the members who joined the government committee ‘Studies on PAPRs’ for 3 years from 2000 to 2002.

REFERENCES

Aero-medical Research Laboratory, Japan Air Self-Defense Force (1972) Body Dimensions of Japan Air Self–Defense Force, Ergonomic Data for the Design of Equipment (1972).

Bergman M, Basu R, Lei Z, Niezgoda G and Zhuang Z (2017), Development of a Manikin-Based Performance Evaluation Method for Loose-Fitting Powered Air-Purifying Respirators, J. Int. Soc. Resp. Protect. 34(1):40-57.

British Standards Institution (2008) BS/EN 12941:1998+A2:2008 Respiratory protective devices – Powered filtering devices incorporating a helmet or a hood – Requirements, testing, marking.

British Standards Institution (2008) BS/EN 12942:1998+A2:2008 Respiratory protective devices – Powered filtering devices incorporating full face masks, half masks or quarter masks – Requirements, testing, marking.

Haruta H, Yuasa H, Shimizu E, Kimura K, Emi H, Nozaki K, Kabe I, Tanaka S (2012), Estimation of Work Rate in Workplaces through the use of Breathing Data, Kokyu-Hogo (Journal on Respiratory Protection in Japanese) vol.24, No.2, 2-12.

ISO/TS16976-1:2015 Respiratory protective devices – Human factors – Part 1: Metabolic rates and respiratory flow rates.

Japanese Industrial Standard Committee (1991), JIS T 8157:1991 Powered Air Purifying Respirators

(Japanese), Japanese Standard Association.

Japanese Industrial Standard Committee (2009), JIS T 8157:2009 Powered Air Purifying Respirators (English), Japanese Standard Association

Matsumura Y, Suzuki K, Ogawa A and Iijima N (2008), Robotic Torso for Inward Leakage Test of PAPR, The 14th International Conference, Abstract Book A30, International Society for Respiratory Protection (2008).

Ministry of Health, Labour and Welfare (2014), Ministerial Notification No.455, 2014, Standard of PAPR (in Japanese), November 28th, 2014.

Ministry of Labour, Japan (1988), Ministerial Notification No.19, 1988, Standard of Particle Respirators (in Japanese), March 30th, 1988.

SIBATA Scientific Technology Ltd. (2015), Specification of Robotic Mannequin Type PR-01(in Japanese).

Technology Institution of Industrial Safety (TIIS) (2002), Committee Report of the Investigation on Powered Air Purifying Respirators (in Japanese).

Yuasa H, Shimizu E, Kimura K, Emi H and Nozaki K (2008) Performance of Breath-Synchronized Powered Air-Purifying Respirator under Simulated Usage Conditions, J. Int. Soc. Resp. Protect. 25 (Issues III & IV): 107-118.